

# The Crystal and Magnetic Structures of $\text{Ba}_3\text{NiRu}_2\text{O}_9$ , $\text{Ba}_3\text{CoRu}_2\text{O}_9$ , and $\text{Ba}_3\text{ZnRu}_2\text{O}_9$

P. LIGHTFOOT<sup>1</sup> AND P. D. BATTLE<sup>2</sup>

*School of Chemistry, University of Leeds, Leeds LS2 9JT,  
United Kingdom*

Received March 6, 1990

The crystal structures of the 6H perovskites  $\text{Ba}_3\text{NiRu}_2\text{O}_9$ ,  $\text{Ba}_3\text{ZnRu}_2\text{O}_9$ , and  $\text{Ba}_3\text{CoRu}_2\text{O}_9$  have been refined from neutron powder diffraction data collected at 5 or 2 K.  $\text{Ba}_3\text{NiRu}_2\text{O}_9$  and  $\text{Ba}_3\text{ZnRu}_2\text{O}_9$  have hexagonal symmetry, space group  $P6_3/mmc$ :  $a_{\text{Ni}} = 5.7256(2)$ .  $c_{\text{Ni}} = 14.0596(2)$  Å;  $a_{\text{Zn}} = 5.7549(2)$ ,  $c_{\text{Zn}} = 14.1328(2)$  Å.  $\text{Ba}_3\text{CoRu}_2\text{O}_9$  undergoes a phase transition from hexagonal symmetry at room temperature to orthorhombic symmetry at 2 K, space group  $Cmcm$ :  $a_{\text{Co}} = 5.7456(1)$ ,  $b_{\text{Co}} = 9.9177(2)$ ,  $c_{\text{Co}} = 14.0862(3)$  Å. In all three compounds the cation sites within the face-sharing octahedra of the 6H structure are occupied by  $\text{Ru}^{5+}$ ; the corner-sharing octahedra are occupied by  $\text{Zn}^{2+}$ ,  $\text{Ni}^{2+}$ , or  $\text{Co}^{2+}$ . The neutron diffraction data show that  $\text{Ba}_3\text{NiRu}_2\text{O}_9$  is magnetically ordered at 5 K, with antiferromagnetic coupling between  $\text{Ru}^{5+}$  ions in the  $\text{Ru}_2\text{O}_9$  dimers and ferromagnetic coupling along approximately linear  $\text{Ni}^{2+}-\text{O}-\text{Ru}^{5+}$  superexchange pathways. The magnetic moments align along  $z$ .  $\text{Ba}_3\text{CoRu}_2\text{O}_9$  is also magnetically ordered with antiferromagnetic coupling in the  $\text{Ru}_2\text{O}_9$  dimers, but in this case antiferromagnetic superexchange between  $\text{Co}^{2+}$  ions leads to a more complex magnetic structure. © 1990 Academic Press, Inc.

## Introduction

Much of our recent research has been concerned with the magnetic properties of  $\text{Ru}^{5+}$  in perovskite-like compounds (1, 2). In this paper we turn our attention to the magnetic properties of the same species in the 6H- $\text{BaTiO}_3$  structure (3). It has been shown (4) that in  $\text{Ba}_3\text{ZnRu}_2\text{O}_9$ ,  $\text{Ba}_3\text{NiRu}_2\text{O}_9$ , and  $\text{Ba}_3\text{CoRu}_2\text{O}_9$  the  $\text{Ru}^{5+}$  ions occupy the face-sharing octahedral sites of the 6H- $\text{BaTiO}_3$  structure, thus forming  $\text{Ru}_2\text{O}_9$  dimers, while the corner-sharing octahedral

sites are occupied by the divalent cation. We have studied these three compounds by neutron powder diffraction in order to explore the magnetic interactions that occur both within and between the dimers. In  $\text{Ba}_3\text{ZnRu}_2\text{O}_9$  the dimers may be considered to be isolated magnetically by the intervening  $\text{ZnO}_6$  octahedra, whereas in  $\text{Ba}_3\text{NiRu}_2\text{O}_9$  and  $\text{Ba}_3\text{CoRu}_2\text{O}_9$  the presence of the paramagnetic species  $\text{Ni}^{2+}$  or  $\text{Co}^{2+}$  increases the likelihood of further, long-range magnetic interaction.

Fernandez *et al.* (5) have undertaken a detailed study of these three phases by  $^{99}\text{Ru}$  Mössbauer spectroscopy. Their results for  $\text{Ba}_3\text{CoRu}_2\text{O}_9$  show the presence of an internal hyperfine field having a strength ( $H_{\text{int}} = 511$  kOe) consistent with the presence of magnetically ordered  $\text{Ru}^{5+}$  at 4.2 K. The

<sup>1</sup> Present address: Materials Science Division, Argonne National Laboratory, Argonne, IL 60439.

<sup>2</sup> To whom correspondence should be addressed at present address: Inorganic Chemistry Laboratory, South Parks Road, Oxford, OX1 3QR, UK.

data for  $\text{Ba}_3\text{NiRu}_2\text{O}_9$  also show a hyperfine field, albeit a weak one ( $H_{\text{int}} = 318$  kOe), and are thus consistent with the existence of long-range antiferromagnetic order, as suggested by the magnetic susceptibility study of Byrne and Moeller (6). The latter observed a complex behavior of  $1/\chi$  vs  $T$  and concluded that the Ni compound is antiferromagnetic below 95 K. They suggested that there may be a ferromagnetic coupling between  $\text{Ru}^{5+}$  and  $\text{Ni}^{2+}$  ( $d^3$ - $d^8$ ) as predicted by Goodenough (7) but these conclusions have never been confirmed by neutron diffraction. In the case of  $\text{Ba}_3\text{ZnRu}_2\text{O}_9$ , Fernandez *et al.* (5) also observed an 18-line pattern at 4.2 K, the linewidths being broad and the magnetic flux density at Ru again being unusually small. This result is more difficult to explain. The observation of magnetic hyperfine splitting in the Mössbauer spectrum implies either the presence of long-range magnetic order despite the replacement of  $\text{Ni}^{2+}$  and  $\text{Co}^{2+}$  by diamagnetic  $\text{Zn}^{2+}$  or a very slow relaxation time for the Ru spins in isolated dimers. A susceptibility study referred to by Fernandez *et al.* (5) apparently revealed a pronounced increase in  $\chi$  at low  $T$ , which cannot be explained on the basis of isolated Ru dimers. Long-range order via Ru-O-Zn-O-Ru superexchange therefore seems to be suggested. However, the Mössbauer spectrum of  $\text{Ba}_3\text{CaRu}_2\text{O}_9$  shows no hyperfine splitting and is consistent with the presence of isolated  $\text{Ru}_2\text{O}_9$  dimers. The absence of long-range magnetic order in the Ca compound has been confirmed in neutron scattering experiments (8) but the true nature of the zinc compound has not been clarified in this way.

## Experimental

Approximately 10 g polycrystalline batches of  $\text{Ba}_3\text{ZnRu}_2\text{O}_9$ ,  $\text{Ba}_3\text{CoRu}_2\text{O}_9$ , and  $\text{Ba}_3\text{NiRu}_2\text{O}_9$  were prepared from appropriate stoichiometric mixtures of  $\text{BaCO}_3$ ,  $\text{ZnO}$ ,  $\text{NiO}$ ,  $\text{Co}_3\text{O}_4$ , and dried  $\text{RuO}_2$  (Johnson

Matthey 'Specpure' Reagents). The mixtures were thoroughly ground in an agate mortar, pelleted, and fired in platinum crucibles, initially at 800°C, then to 1200°C at a rate of 1°/min. After regrinding and repelleting the samples were heated for a total of 10 days at 1200°C (Zn) and 1300°C (Ni and Co) with two intermediate regrindings. Room-temperature X-ray powder diffraction patterns of all three products could be indexed on the basis of a 6H-BaTiO<sub>3</sub>-like hexagonal unit cell. Neutron diffraction data were collected at 5 K (Ni and Zn) or 2 K (Co) on the medium resolution diffractometer D1a and ILL, Grenoble. Samples were contained in thin-walled vanadium cans and held in a cryostat with an Al tail. Data were collected at  $2\theta$  intervals of 0.05° over the angular range  $0 < 2\theta < 156$ , each experiment taking approximately 11 hr.

## Results

Profile analysis of the diffraction data was carried out by the Rietveld (9) method, assuming a Gaussian shape for the Bragg peaks and using the following coherent scattering lengths:  $b(\text{Ba}) = 0.52$ ,  $b(\text{Zn}) = 0.57$ ,  $b(\text{Ni}) = 1.03$ ,  $b(\text{Co}) = 0.25$ ,  $b(\text{Ru}) = 0.73$ ,  $b(\text{O}) = 0.58 \times 10^{-12}$  cm. The background level was estimated by interpolation between regions of the profile where there were no Bragg peaks, and statistical variations were taken into account in assigning a weight to each profile point. The starting model for the refinement of all three structures was the structure of  $\text{Ba}_3\text{NiSb}_2\text{O}_9$  as determined by Jacobson and Calvert (10), with Ru occupying the cation positions in the face-sharing octahedra, and Ni, Zn, or Co occupying the vertex-sharing sites.

### (i) Structure Refinement of $\text{Ba}_3\text{NiRu}_2\text{O}_9$ and $\text{Ba}_3\text{ZnRu}_2\text{O}_9$

Initially it was assumed that there was no magnetic scattering in the data. Refinements

of the nuclear structures in space group  $P6_3/mmc$  (giving a total of 18 variable parameters) converged smoothly to agreement factors  $R_{wp} = 8.62\%$ ,  $R_1 = 2.9\%$ ,  $R_{exp} = 3.95\%$  for  $Ba_3ZnRu_2O_9$ , and  $R_{wp} = 9.90\%$ ,  $R_1 = 3.47\%$ ,  $R_{exp} = 2.73\%$  for  $Ba_3NiRu_2O_9$ . No evidence was found either for disorder of  $Ru/M^{2+}$  over their respective sites or for partial occupancy of the oxygen sites. It was apparent at this stage, however, that a small amount of additional (magnetic) scattering was present in the case of the Ni compound. The predicted (7)  $Ru^{5+}-O-Ru^{5+}$  90° superexchange is antiferromagnetic, whereas that predicted for a 180°  $Ni^{2+}-O-Ru^{5+}$  pathway is ferromagnetic. The magnetic model drawn (12) in Fig. 3 is consistent with these predictions and was therefore tested for  $Ba_3NiRu_2O_9$ . The model is composed of ferromagnetic sheets of  $Ni^{2+}$  ions, each of which is coupled ferromagnetically to six  $Ru^{5+}$  ions in different  $Ru_2O_9$  dimers; the antiferromagnetic coupling within each dimer ensures that successive  $Ni^{2+}$  layers have opposite spin directions. The  $Ni^{2+}$  and  $Ru^{5+}$  magnetic moments were constrained to lie along the  $z$  axis of the hexagonal unit cell. The free-ion form factor for  $Ni^{2+}$  was taken from Watson and Freeman (11), while the curve derived during a study of  $Sr_2ErRuO_6$  (13) was used for  $Ru^{5+}$ . This model refined to give reasonable values for the magnetic moments on both cations ( $\mu_{Ru} = 1.5(2)$ ,  $\mu_{Ni} = 1.7(1)$   $\mu_B$ ), and a significant improvement in the overall profile fit ( $R_{wp} = 9.56\%$ ,  $R_1 = 3.11\%$ ,  $R_{mag} = 12.6\%$ ). Attempted refinements with the Ni-O-Ru interaction antiferromagnetic, or with the moments constrained to lie in the  $xy$  plane, gave poorer fits. Magnetic models for  $Ba_3ZnRu_2O_9$ , with antiferromagnetic intracluster interactions and either ferro- or antiferromagnetic intercluster interactions, did not lead to significant improvements in the overall fits, and on this basis we conclude that any long-range magnetic order present in this compound requires an ordered moment

of no more than 0.4  $\mu_B$  per  $Ru^{5+}$ . The final observed, calculated, and difference diffraction profiles are plotted in Figs. 1 and 2 for  $Ba_3NiRu_2O_9$  and  $Ba_3ZnRu_2O_9$ , respectively.

### (ii) Structure Refinement of $Ba_3CoRu_2O_9$

The appearance of the diffraction pattern of  $Ba_3CoRu_2O_9$  was very different from that of  $Ba_3NiRu_2O_9$ . In order to index all the Bragg peaks, it was necessary to lower the symmetry from hexagonal to orthorhombic, using a primitive unit cell having  $a = 5.7456(1)$ ,  $b = 9.9177(2)$ , and  $c = 14.0862(3)$  Å, i.e.,  $a_{ortho} \sim a_{hex}$ ,  $b_{ortho} \sim \sqrt{3}b_{hex}$ ,  $c_{ortho} \sim c_{hex}$ . In devising a magnetic structure consistent with this symmetry we again made the assumption that the magnetic coupling within the  $Ru_2O_9$  dimers would be antiferromagnetic. Furthermore, because the crystal structure of a 6H perovskite is C-centered in this orthorhombic unit-cell (space group  $Cmcm$ ) we assumed that the reflections having  $h + k = 2n + 1$  must be magnetic in origin, i.e., the C-centering is absent from the origin, i.e., the C-centering is absent from the origin, i.e., the C-centering is absent from the origin. A structure consistent with these conditions is drawn in Fig. 4. Each Co atom is coupled to six others along a superexchange pathway of the form Co-O-Co. Of these six linkages, four are antiferromagnetic and two are ferromagnetic; the distance between antiferromagnetically coupled Co atoms being slightly shorter than that between ferromagnetic pairs. Each Ru atom is coupled to three Co atoms via a Ru-O-Co linkage; two of these interactions are ferromagnetic, the third is antiferromagnetic. The superexchange within the  $Ru_2O_9$  dimers is always antiferromagnetic as required. Subsequent profile analysis showed that this is a valid model for the crystal and magnetic structures of  $Ba_3CoRu_2O_9$ , with refinements of 13 atomic parameters, an overall temperature factor, the ordered magnetic moments of the  $Ru^{5+}$  and  $Co^{2+}$  ions, and the usual profile parameters converging to the following agreement factors:  $R_{wpr} = 11.8\%$ ,  $R_1 = 4.7\%$ ,  $R_{mag} =$

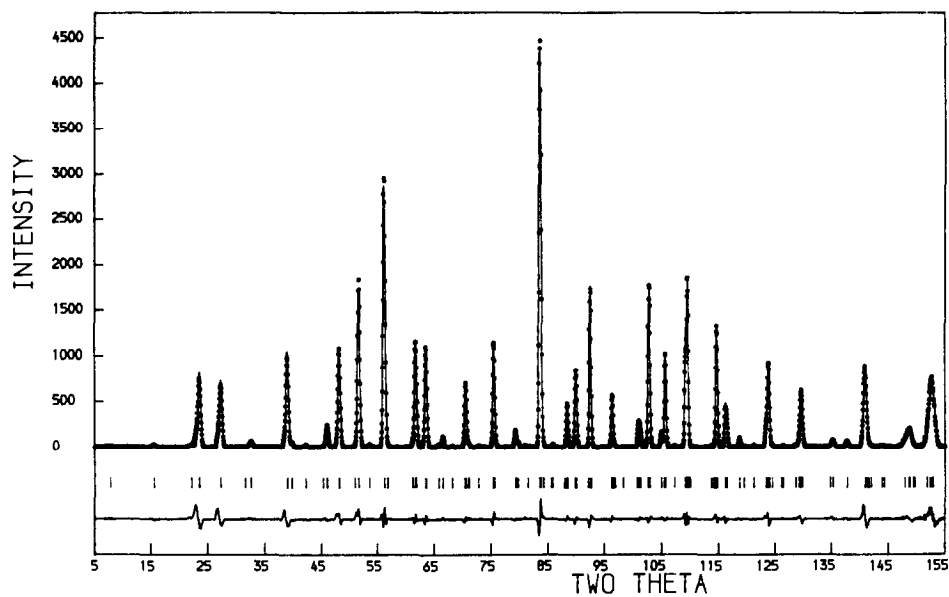


FIG. 1. The observed, calculated, and difference neutron powder diffraction profiles of  $\text{Ba}_3\text{NiRu}_2\text{O}_9$  at 5 K. Reflection positions are marked.

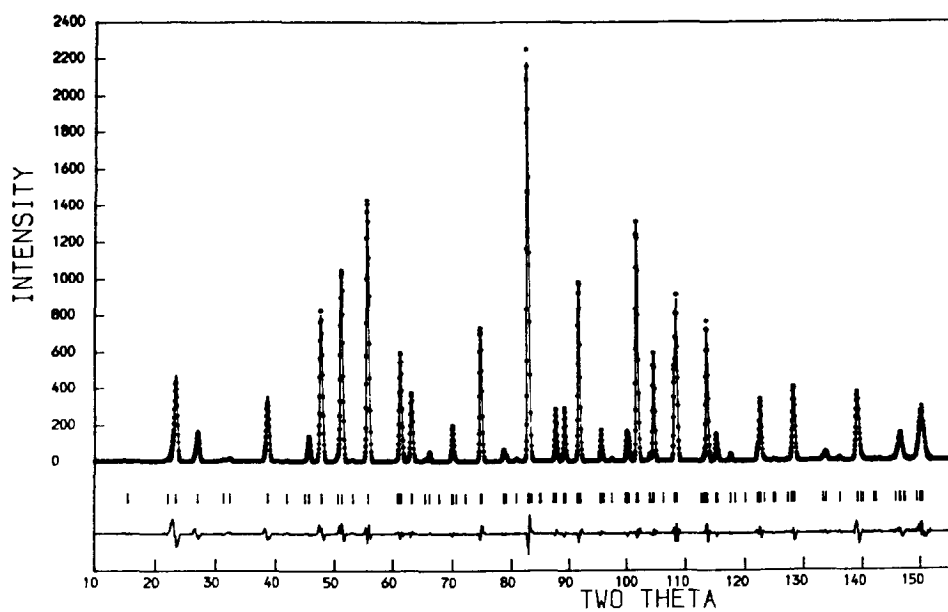


FIG. 2. The observed, calculated, and difference neutron powder diffraction profiles of  $\text{Ba}_3\text{ZnRu}_2\text{O}_9$  at 5 K. Reflection positions are marked.

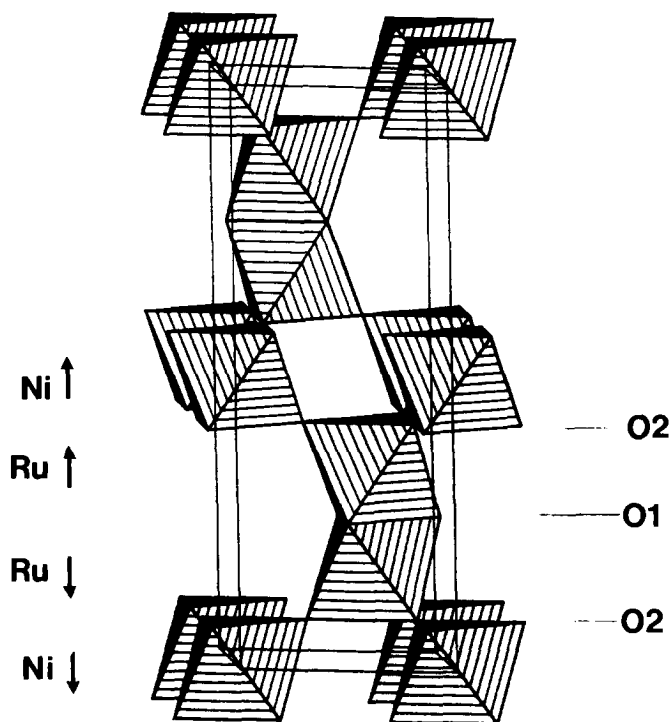


FIG. 3. The crystal structure of  $Ba_3MRu_2O_9$  ( $M = Ni$  or  $Zn$ ) with Ba atoms omitted. The directions of the ordered atomic magnetic moments in  $Ba_3NiRu_2O_9$  are shown.

29.8%. The final observed, calculated, and difference diffraction profiles are drawn in Fig. 5. The most obvious discrepancy, a sharp peak at  $2\theta \sim 84^\circ$ , is likely to be a (220) reflection from the Al cryostat which was left unshielded during the collection of this particular data set. The relatively high magnetic  $R$ -factor is a reflection of the weakness of the magnetic scattering. The ordered magnetic moments of the  $Co^{2+}$  and  $Ru^{5+}$  ions were found to lie along the  $y$  axis of the unit cell with refined magnitudes of 2.71(5) and 1.44(5)  $\mu_B$ , respectively, when the free ion form factor (11) was used for  $Co^{2+}$ .

### Discussion

The refined atomic coordinates and bond distances/angles for  $Ba_3ZnRu_2O_9$  (Tables I and II) and  $Ba_3NiRu_2O_9$  (Tables III and IV)

confirm the basic structural features of the proposed 6H- $BaTiO_3$  structure. Ru exclusively occupies the face-sharing octahedral sites in both cases, with the metal atoms being displaced away from the centers of the octahedra in opposite directions to give Ru-Ru distances of 2.685 and 2.681 Å in  $Ba_3ZnRu_2O_9$  and  $Ba_3NiRu_2O_9$ , respectively. It may also be noted that the O(1)-O(1) distances within the shared face are comparatively short, at 2.641 and 2.634 Å, respectively, thus helping to 'shield' the  $Ru^{5+}$ - $Ru^{5+}$  repulsion. The average Ru-O bond length of 1.965 Å is very similar to that found in other  $Ru^{5+}$  oxides (2, 14, 15), although the  $RuO_6$  octahedra are less regular than those reported previously.

Although  $Ba_3CoRu_2O_9$  undergoes a transformation to orthorhombic symmetry between room temperature and 2 K, the crys-

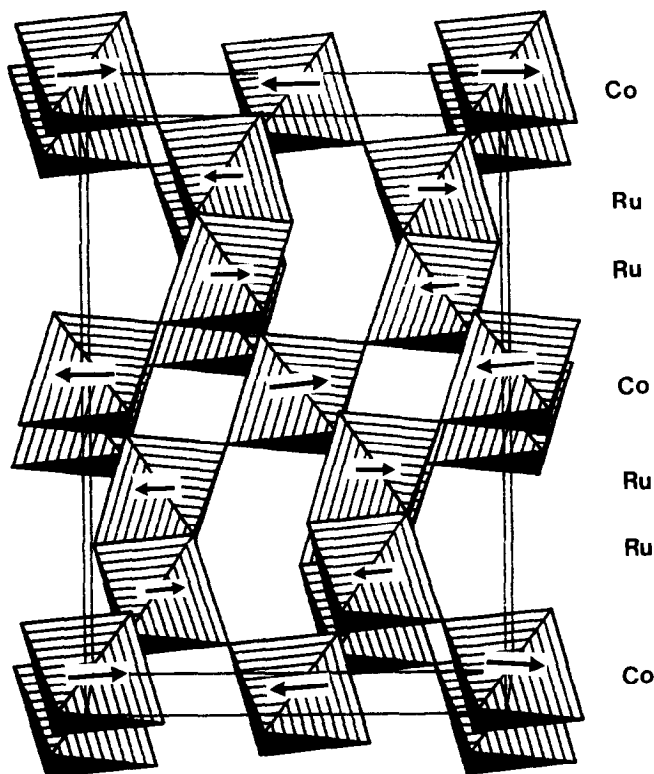


FIG. 4. The crystal and magnetic structures of  $\text{Ba}_3\text{CoRu}_2\text{O}_9$  viewed along  $x$ . The directions of the ordered magnetic moments are shown.

tal structure is still essentially that of a 6H hexagonal perovskite, as can be seen from Fig. 4 and the atomic parameters and bond distances presented in Tables V and VI. The shortest Ru–Ru distance is 2.677 Å and once

again the oxygen–oxygen distances within the shared octahedral face are relatively short at 2.67 Å (O1–O2). There are now four different Ru–O distances in the first coordination shell of the transition metal,

TABLE I  
STRUCTURAL PARAMETERS FOR  $\text{Ba}_3\text{ZnRu}_2\text{O}_9$  AT 5 K (SPACE GROUP  $P6_3/mmc$ )

Atom	Site	$x$	$y$	$z$	$B_{\text{iso}}$ ( $\text{\AA}^2$ )
Ba1	2b	0	0	1/4	0.12(7)
Ba2	4f	1/3	2/3	0.9101(2)	0.08(6)
Ni	2a	0	0	0	0.18(7)
Ru	4f	1/3	2/3	0.1551(1)	0.16(4)
O1	6h	0.4864(3)	-0.0273(5)	1/4	0.29(4)
O2	12k	0.1715(2)	0.3430(4)	0.41571(9)	0.25(3)

Note.  $a = 5.7549(2)$ ,  $c = 14.1328(2)$  Å.

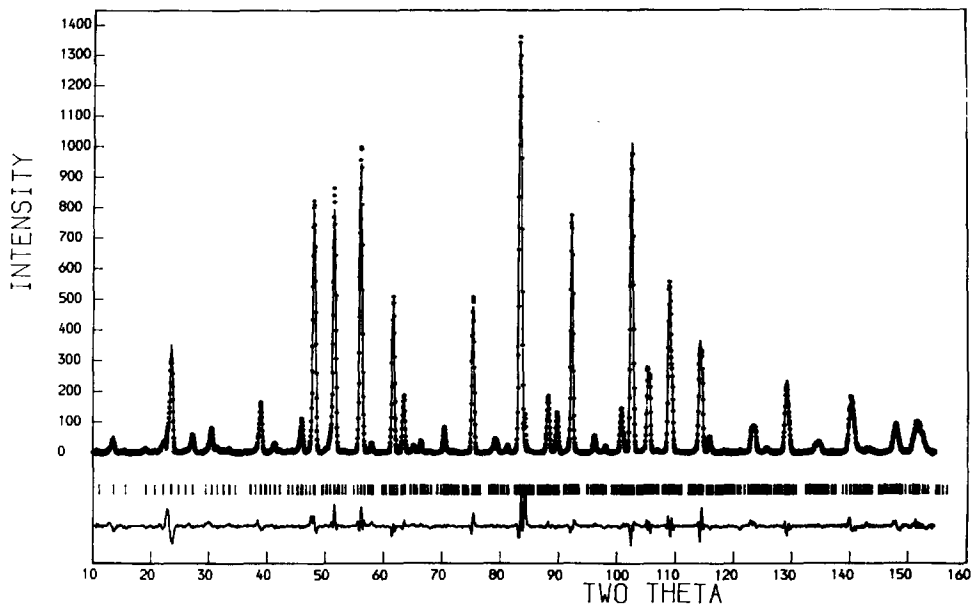


FIG. 5. The observed, calculated, and difference neutron powder diffraction profiles of  $\text{Ba}_3\text{CoRu}_2\text{O}_9$  at 2 K. Reflection positions are marked.

but they fall into two distinct groups, as found in the hexagonal Ni and Zn analogues.

Our neutron diffraction data prove that  $\text{Ba}_3\text{NiRu}_2\text{O}_9$  is antiferromagnetic at 5 K, as has been suggested previously on the basis of Mössbauer and susceptibility data. The ordered magnetic moment of the  $\text{Ru}^{5+}$  ions is somewhat smaller than the value of ca.

$1.9 \mu_B$  found previously in cubic and pseudocubic perovskites (12, 14), although a value of only  $1.2 \mu_B$  was found in  $\text{Ca}_2\text{YRuO}_6$  (15). The magnetic moment of  $1.7(1) \mu_B$  found for  $\text{Ni}^{2+}$  in this work is only slightly lower than that found in other  $\text{Ni}^{2+}$  oxides (16). Inadequacies in the chosen form factors may, in part, account for these reductions, but it is worth noting that the hyperfine field measured in the Mössbauer study of  $\text{Ba}_3\text{NiRu}_2\text{O}_9$  was anomalously low.  $\text{Ba}_3\text{NiRu}_2\text{O}_9$  is the first compound containing  $\text{Ru}_2\text{O}_9$  dimers in which the presence of long-range magnetic order has been proved by neutron diffraction, although spin pairing within individual dimers is well-established (17). The observation of ferromagnetic coupling between  $\text{Ru}^{5+}$  and  $\text{Ni}^{2+}$  was postulated by Byrne and Moeller (6) in the interpretation of their magnetic susceptibility data. The strength of this interaction will be enhanced by the almost-linear Ni-O-Ru superexchange pathway ( $\text{Ni}\hat{\text{O}}\text{Ru} = 177.2^\circ$ ). Similar

TABLE II  
BOND LENGTHS (Å) AND BOND ANGLES ( $^\circ$ )  
IN  $\text{Ba}_3\text{ZnRu}_2\text{O}_9$  AT 5 K

Ba1-O1	$2.881(3) \times 6$	Ba2-O1	$2.891(4) \times 3$
Ba1-O2	$2.899(3) \times 6$	Ba2-O2	$2.879(4) \times 6$
		Ba2-O2'	$2.943(4) \times 3$
Zn-O2	$2.083(3) \times 6$	Ru-O1	$2.032(4) \times 3$
Ru-Ru'	$2.685(2)$	Ru-O2	$1.898(3) \times 3$
O1-O1	$2.641(5) \times 2$	O1-O2	$2.820(4) \times 4$
O1-O1'	$3.114(5) \times 2$		
O2-Zn-O2	90.6	O1-Ru-O1'	81.1
Zn-O2-Ru	176.9	O1-Ru-O2	170.4
		O2-Ru-O1	91.7

TABLE III  
STRUCTURAL PARAMETERS FOR Ba<sub>3</sub>NiRu<sub>2</sub>O<sub>9</sub> AT 5 K (SPACE GROUP P6<sub>3</sub>/mmc)

Atom	Site	<i>x</i>	<i>y</i>	<i>z</i>	<i>B</i> <sub>iso</sub> (Å <sup>2</sup> )	μ  (μ <sub>B</sub> )
Ba1	2 <i>b</i>	0	0	1/4	0.00(8)	
Ba2	4 <i>f</i>	1/3	2/3	0.9110(2)	0.10(7)	
Ni	2 <i>a</i>	0	0	0	0.20(4)	1.7(1)
Ru	4 <i>f</i>	1/3	2/3	0.1546(1)	0.18(5)	1.5(2)
O1	6 <i>h</i>	0.4867(3)	-0.0266(6)	1/4	0.27(4)	
O2	12 <i>k</i>	0.1708(2)	0.3415(4)	0.4170(1)	0.15(3)	

Note. *a* = 5.7256(2), *c* = 14.0596(2) Å.

ferromagnetic coupling has also been proposed to account for the unusual magnetic properties of the perovskite BaLaNiRuO<sub>6</sub> (*I*). The alignment of the spins along *z* rather than in *xy* plane is perhaps due to the second order spin-orbit coupling associated with both Ni<sup>2+</sup> and Ru<sup>5+</sup>, although likely to be stronger in the latter.

The difference between the magnetic structures of Ba<sub>3</sub>NiRu<sub>2</sub>O<sub>9</sub> and Ba<sub>3</sub>CoRu<sub>2</sub>O<sub>9</sub> is quite striking. Our results show that both compounds exhibit antiferromagnetic coupling within the Ru<sub>2</sub>O<sub>9</sub> dimers, but that the magnetic ordering observed among the divalent cations is quite different in the two cases. This presumably stems from the fact that the *t*<sub>2g</sub> orbitals are not completely filled in the case of Co<sup>2+</sup>, thus increasing the strength of the antiferromagnetic *M*<sup>2+</sup>-O-O-*M*<sup>2+</sup> superexchange within the

layers of corner-sharing octahedra which lie perpendicular to the *z* axis (Fig. 4). The filled *t*<sub>2g</sub> orbitals of Ni<sup>2+</sup> cannot take part in such an interaction, and we therefore find ferromagnetic layers in Ba<sub>3</sub>NiRu<sub>2</sub>O<sub>9</sub>, thus maximizing the number of ferromagnetic, ~180° Ni- $\hat{O}$ -Ru linkages. The Co-O-Ru superexchange pathways are also almost linear (Ru- $\hat{O}$ 3-Co = 176.8°, Ru- $\hat{O}$ 4-Co = 177.2°) and so ferromagnetic coupling between Ru and Co is predicted in Ba<sub>3</sub>CoRu<sub>2</sub>O<sub>9</sub>. However, the antiferromagnetic Co-O-O-Co coupling and the ferromagnetic Co-O-Ru coupling cannot be completely satisfied simultaneously, and the re-

TABLE V  
STRUCTURAL PARAMETERS FOR Ba<sub>3</sub>CoRu<sub>2</sub>O<sub>9</sub> AT 2 K  
(SPACE GROUP *Cmcm*)

Atom	Site	<i>x</i>	<i>y</i>	<i>z</i>	μ  (μ <sub>B</sub> )
Ba1	4 <i>c</i>	0	0.000(1)	1/4	
Ba2	8 <i>f</i>	0	0.3342(8)	0.0897(2)	
Co	4 <i>a</i>	0	0	0	2.71(4)
Ru	8 <i>f</i>	0	0.3284(5)	0.8450(1)	1.44(5)
O1	4 <i>c</i>	0	0.5136(9)	1/4	
O2	8 <i>g</i>	0.270(1)	0.2477(6)	1/4	
O3	8 <i>f</i>	0	0.8335(6)	0.0833(8)	
O4	16 <i>h</i>	0.2547(9)	0.0892(5)	0.0833(4)	

Note. Overall *B*<sub>iso</sub> = 0.13(3) Å<sup>2</sup>. *a* = 5.7456(1), *b* = 9.9177(2), *c* = 14.0862(3) Å.

TABLE IV  
BOND LENGTHS (Å) AND BOND ANGLES (°)  
IN Ba<sub>3</sub>NiRu<sub>2</sub>O<sub>9</sub> AT 5 K

Ba1-O1	2.866(4) × 6	Ba2-O1	2.883(5) × 3
Ba1-O2	2.895(3) × 6	Ba2-O2	2.864(4) × 6
		Ba2-O2'	2.906(4) × 3
Ni-O2	2.056(3) × 6	Ru-O1	2.027(4) × 3
Ru-Ru'	2.681(2)	Ru-O2	1.902(3) × 3
O1-O1	2.634(5) × 2	O1-O2	2.824(5) × 4
O1-O1'	3.091(5) × 2		
O2-Ni-O2	90.9	O1-Ru-O1'	81.0
Ni-O2-Ru	177.2	O2-Ru-O1	91.9
		O1-Ru-O2	170.6



TABLE VI  
BOND LENGTHS (Å) AND BOND ANGLES (°)  
IN Ba<sub>3</sub>CoRu<sub>2</sub>O<sub>9</sub> AT 2 K

Ba1-O1	2.88(1) × 2	Ba2-O1	2.88(1)
Ba1-O2	2.90(1) × 2	Ba2-O2	2.87(1) × 2
Ba1-O2'	2.83(1) × 2	Ba2-O3	2.95(2)
Ba1-O3	2.87(1) × 2	Ba2-O3'	2.87(2) × 2
Ba1-O4	2.91(1) × 4	Ba2-O4	2.84(1) × 2
		Ba2-O4'	2.90(1) × 2
		Ba2-O4''	2.92(1) × 2
Co-O3	2.03(1) × 2	Ru-O1	2.06(1)
Co-O4	2.074(9) × 4	Ru-O2	2.03(1) × 2
		Ru-O3	1.90(1)
Ru-Ru	2.677(7)	Ru-O4	1.92(1) × 2
O1-O2	3.06(1) × 2	O2-O2	3.10(1)
O1-O2'	2.67(1) × 2	O2-O2'	2.64(1)
O1-O4	2.84(1) × 4	O2-O3	2.83(2) × 2
		O2-O4	2.83(1) × 2
O3-O4	2.93(2) × 2	O4-O4	2.94(1)
O3-O4'	2.87(2) × 2	O4-O4'	2.93(1)
O4-O4''	2.80(2) × 2	O4-O4''	2.82(1)
O3-Co-O3	180.0	O1-Ru-O2	81.6
O3-Co-O4	91.2	O1-Ru-O3	171.7
O4-Co-O4	90.2	O1-Ru-O4	91.0
		O2-Ru-O3	92.1
Ru-O3-Co	176.8	O2-Ru-O4	91.6
Ru-O4-Co	177.2	O2-Ru-O4'	170.5
		O3-Ru-O4	94.6

sultant structure represents a compromise in which 2/3 of the Ru-O-Co couplings are ferromagnetic, 1/3 antiferromagnetic, whereas 2/3 of the Co-O-O-Co couplings are antiferromagnetic, 1/3 ferromagnetic. The antiferromagnetic coupling in the latter case is stabilized by the orthorhombic distortion, which reduces the distance between antiferromagnetic Co pairs. The magnitude of the ordered magnetic moment of the Ru<sup>5+</sup> ions in Ba<sub>3</sub>CoRu<sub>2</sub>O<sub>9</sub> is similar to values reported previously (2, 14, 15) whereas the value of 2.7 μ<sub>B</sub> found for Co<sup>2+</sup> is perhaps lower than expected for an ion with a 3d<sup>7</sup> electron configuration. It may be that the reduction in site symmetry has essentially quenched any orbital contribution to the magnetic moment. Alternatively, the low value of the moment (and the high value of R<sub>magn</sub>) may arise from the use of a collinear-spin model for the magnetic structure.

Our failure to detect any magnetic Bragg scattering in the diffraction pattern of Ba<sub>3</sub>ZnRu<sub>2</sub>O<sub>9</sub> indicates that there is no long-

range magnetic order in this compound at 5 K. This is consistent with the suggestion by Fernandez *et al.* (5) that the Neel temperature of Ba<sub>3</sub>ZnRu<sub>2</sub>O<sub>9</sub> is only slightly higher than 4.2 K. The weak hyperfine field and the relatively large linewidths observed in the Mössbauer data collected at that temperature can then be explained as arising from an unsaturated spin system displaying time-dependent relaxation phenomena just below the ordering temperature. Further neutron diffraction experiments at lower temperatures are needed to confirm this model. Finally, we note that this interpretation of our neutron data gives no explanation for the anomalous increase in magnetic susceptibility which occurs for many of these hexagonal Ru<sup>5+</sup> perovskites at very low temperatures. The cause of this increase is still uncertain.

### Acknowledgments

We are grateful to the SERC for the award of a Postdoctoral Research Assistantship (P.L.) and for the provision of neutron scattering facilities at ILL Grenoble. We thank Dr. J. K. Cockcroft for his assistance during our visit to ILL.

### References

1. P. D. BATTLE, T. C. GIBB, C. W. JONES, AND F. STUDER, *J. Solid State Chem.* **78**, 281 (1989).
2. P. D. BATTLE AND C. W. JONES, *J. Solid State Chem.* **78**, 108 (1989).
3. R. D. BURBANK AND H. T. EVANS, *Acta Crystallogr.* **1**, 330 (1948).
4. P. C. DONOHUE, L. KATZ, AND R. WARD, *Inorg. Chem.* **5**, 339 (1966).
5. I. FERNANDEZ, R. GREATREX, AND N. N. GREENWOOD, *J. Solid State Chem.* **34**, 121 (1980).
6. R. C. BYRNE AND C. W. MOELLER, *J. Solid State Chem.* **2**, 228 (1970).
7. J. B. GOODENOUGH, "Magnetism and the Chemical Bond," Interscience, New York (1963).
8. J. DARRIET, J. L. SOUBEYROUX, AND A. P. MURANI, *J. Phys. Chem. Solids* **44**, 269 (1983).
9. H. M. RIETVELD, *J. Appl. Crystallogr.* **2**, 65 (1969).
10. A. J. JACOBSON AND A. J. CALVERT, *J. Inorg. Nucl. Chem.* **40**, 447 (1978).

11. R. E. WATSON AND A. J. FREEMAN, *Acta Crystallogr.* **14**, 27 (1961).
12. R. X. FISCHER, *J. Appl. Crystallogr.* **18**, 258 (1985).
13. P. D. BATTLE AND C. W. JONES, to be published.
14. P. D. BATTLE AND W. J. MACKLIN, *J. Solid State Chem.* **52**, 138 (1984).
15. P. D. BATTLE AND W. J. MACKLIN, *J. Solid State Chem.* **54**, 245 (1984).
16. H. A. ALPERIN, *J. Phys. Soc. Japan, Suppl. BIII* **17**, 12 (1962).
17. J. DARRIET, M. DRILLON, G. VILLENEUVE, AND P. HAGENMULLER, *J. Solid State Chem.* **19**, 213 (1976).